Arktos (2015) 1:9
DOI 10.1007/s41063-015-0016-6

ORIGINAL ARTICLE

Age and composition of basement beneath the De Long archipelago, Arctic Russia, based on zircon U–Pb geochronology and O–Hf isotopic systematics from crustal xenoliths in basalts of Zhokhov Island

Viacheslav V. Akinin[1] · Eric S. Gottlieb[2] · Elizabeth L. Miller[2] · Gennady O. Polzunenkov[1] · Nikolay M. Stolbov[3] · Nikolay N. Sobolev[4]

Received: 28 August 2015 / Accepted: 7 October 2015 / Published online: 20 November 2015

Abstract U–Pb ages, in conjunction with oxygen isotope and hafnium isotope geochemistry of zircons from granitic and siliciclastic crustal xenoliths from Cenozoic alkali basalts on Zhokhov Island (De Long Archipelago, Russian Arctic), provide new insights about the island's subsurface geology. Zircons from granitic gneiss xenoliths yield $^{206}Pb/^{238}U$ ages ranging from 600 to 660 Ma, similar to protolith ages of granite intrusions and orthogneisses in Protouralian–Timanian magmatic basement of the northern Urals as well as to rocks that form the basement of Arctic Chukotka and Wrangel Island, thus suggesting continuity between these three regions. Depleted mantle-like Hf and O isotopic signatures in the dated zircons suggest juvenile crust that originally formed in the Neoproterozoic and was later reworked during the Paleozoic and Mesozoic. Sandstone xenoliths contain detrital zircon (DZ) populations that establish their depositional age as younger than Permian and reveal similarities to DZ populations of Permian and Triassic strata of Taimyr and Chukotka.

✉ Viacheslav V. Akinin
akinin@neisri.ru

[1] North-East Interdisciplinary Scientific Research Institute, Far East Branch- Russian Academy of Sciences, 16 Portovaya Street, 685000 Magadan, Russia

[2] Department of Geological Sciences, Stanford University, 450 Serra Mall, Bldg. 320, Stanford, CA, USA

[3] FSUE "VNIIOkeangeologia named after I.S. Gramberg", 1, Angliysky Avenue, St. Petersburg 190121, Russia

[4] Federal State Unitary Enterprise, "A. P. Karpinsky Russian Geological Research Institute" (FGUP «VSEGEI»), 74, Sredny Prospect, 199106 St. Petersburg, Russia

Keywords Crustal xenoliths · Zircon geochronology · Hf isotopes · De Long · Circum-Arctic tectonics

Introduction and previous work

The De Long archipelago in the East Siberian Sea consists of several small islands (Zhokov, Jeannette, Henrietta, Bennett, and Vil'kitskiy) that are the northeastern most landmasses of the New Siberian Islands and have been included within the northwestern edge of the composite Arctic Alaska–Chukotka crustal terrane (AACH) (e.g., [3] (Fig. 1). Determining the age and composition of basement of the AACH terrane has been a fundamental challenge in understanding the plate tectonic history of this vast, remote, and largely submerged crustal block, and thus bedrock exposures in the De Long archipelago provide invaluable data for addressing this problem. Although the oldest metamorphic rocks from AACH were shown as Archean on Russian geologic maps until the early 1990s, sparse U–Pb geochronology data from outcrops on Wrangel Island, Chukotka Peninsula, and Seward Peninsula indicate AACH crust is significantly younger, generally consisting of Meso- and Neoproterozoic basement covered by Paleozoic and Mesozoic strata [2, 6, 9, 17]. The first-reported U–Pb geochronology studies of rocks of the De Long archipelago have suggested a correlation with the Timanides of Baltica (Polar Urals) as well as the rest of the AACH on the basis of late Neoproterozoic age results from igneous samples [4, 8].

Although Zhokhov Island (152°42′E, 76°08′N; Fig. 1) within the De Long archipelago is nearly entirely covered by late Neogene to Quaternary alkali basalts, the basalts entrain an assortment of crustal and mantle xenoliths [19, 20]. We collected xenoliths of granitic gneiss and

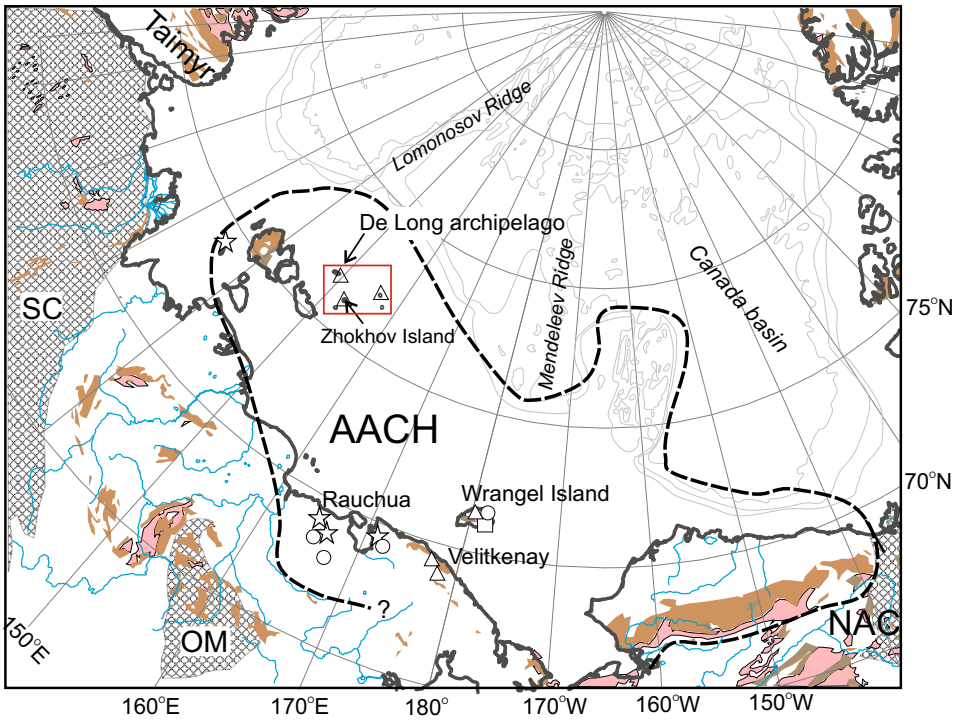

Fig. 1 Location of samples discussed in text. *Net pattern* shows ancient Archean cratons in circum-Arctic: Siberian craton (SC), Omolon block (OM), North American craton (NAC). Dashed line delineates Arctic Alaska–Chukotka microplate (AACH). *Rose* indicates exposures of Proterozoic rocks, *dark brown*—Paleozoic intrusions, and *light brown*—Paleozoic sedimentary rocks. Location and age of detrital zircons samples compiled on Fig. 4 are symbolized as follows: upper Jurassic-Cretaceous (*open star*), Triassic (*open circle*), Permian-Carboniferous (*squares*), Devonian-Carboniferous (*triangle*) [4, 6, 13, 14]

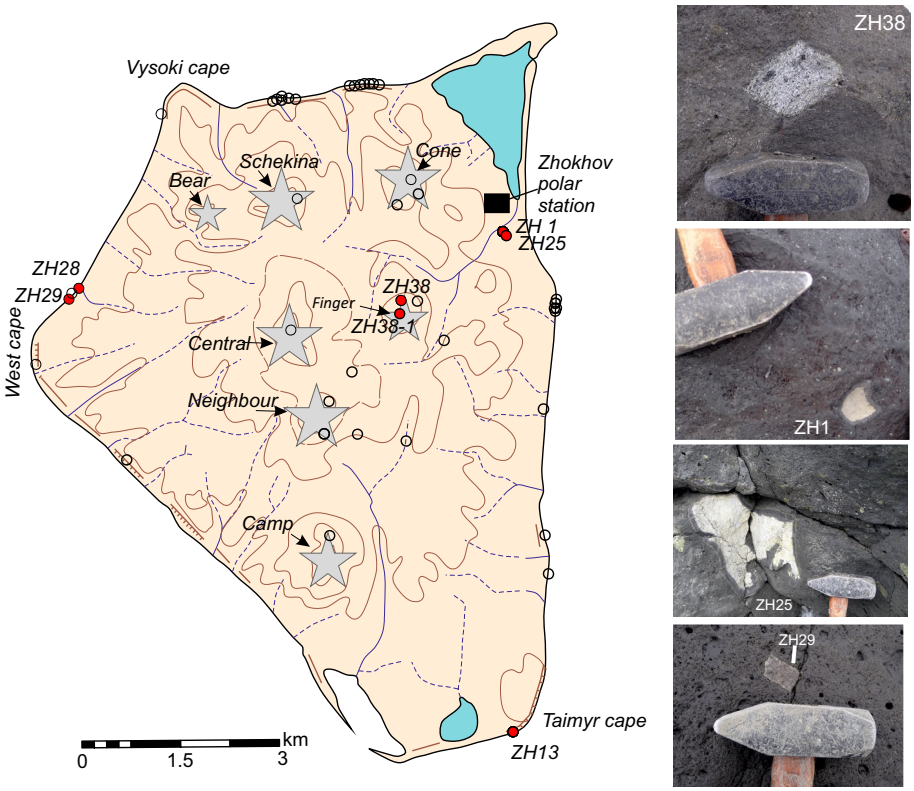

Fig. 2 Simplified geological map of Zhokhov Island. Gray stars are hills reconstructed as volcanic craters. *Yellow*—undivided massive alkali basalt lava flows and scoria. *Filled circles*—crustal xenoliths samples described in this manuscript, *open circles*—locations of other samples collected (mostly alkali basalts and mantle xenoliths). Photographs of outcrops with crustal xenoliths are shown at *right*

sandstone (Fig. 2) from these basalts to gain information about the composition and age of pre-volcanic rock units in the subsurface of Zhokhov Island. The most comprehensive petrological and geochemical study of the alkali basalts and mantle xenoliths of Zhokhov Island was carried out by [20], but that study, which focused primarily

on mantle-derived material, only described one crustal xenolith (a Cretaceous dolerite). The age of eruption of the basalts has been reported as between 1.2 and 10 Ma, and more precise $^{40}Ar/^{39}Ar$ dating of a single sample has yielded an age of 1.2 ± 0.2 Ma [11]. Although not the subject of this paper, the timing of basaltic volcanism on Zhokhov Island is constrained by new K–Ar results as active during the period 1.4 ± 0.1 to 3.6 ± 0.6 Ma (Akinin et al. *in prep*.), which overlaps the Plio-Pleistocene timing of glaciations documented in the Arctic [7]. Thus, the potential for volcanic flows to envelop and transport glacial sediments at the surface cannot be ruled out. However, given that 90–95 % of the xenoliths observed in basalts on Zhokhov are derived from the mantle, it is likely that at least some of the crustal xenoliths in the volcanic strata were incorporated into magmas in the subsurface.

Recent studies [4, 8] present new U–Pb geochronology of acid rocks hosted by Cenozoic basalt on Zhokhov yielding concordant ages of 568 ± 4 and 602 ± 2 Ma [8] and 533 ± 1, 578 ± 2 Ma, and a multimodal result of 638 ± 5 and 663 ± 7 Ma [4], and thus four of five samples yield ages between ca. 530–600 Ma. However, it is uncertain whether these ≤600 Ma samples were transported in magmas that passed *through the crust* or were simply entrained by basalt flows *as they flowed over the land surface*. Given the history of glaciation in the region [7], boulders and cobbles in basalt flows may have been glacially transported vast distances across the Pleistocene Arctic landscape onto Zhokov Island before being incorporated into the basalts, and are thus potentially problematic in terms of being representative of bedrock geology. Here we present U–Pb, O and Lu–Hf isotopic results from zircons from granitic gneiss and sandstone xenoliths that we believe were picked up on the way to the surface and offer some petrologic and paleogeographic interpretations of these data in context of the geology of the AACH crustal block.

Data collection and analytical methods

Twenty-nine samples of crustal xenoliths were collected from different parts of the island. From greatest to least abundant, these consist of gray quartz-feldspar-bearing sandstones, granitic gneisses, marble, plagioclase-amphibole-bearing pegmatites, and diorites. Importantly, we collected crustal xenoliths only within craggy outcrops of basalts at multiple localities across the island (Fig. 2), discriminating them from the possible boulder-size glacial erratics reported upon by Lorenz [12] and Ershova et al. [4]. The diameter of most crustal xenoliths we observed ranges from 2 to 5 cm, with very rare fragments up to 10–15 cm across. We note that the small volumes of the xenolith material collected yielded less zircons in the mineral separates relative to routine geochronology work in which sample volume is not an issue. All crustal xenoliths are classified as fragments of upper crustal rocks likely derived from shallow depths of the underlying basement. No obvious lower crustal xenoliths such as mafic granulites or gabbros as described in Akinin et al. [1] were identified.

Using conventional separation techniques, zircon was separated from eight samples of crustal xenoliths, and 63 grains were dated via Secondary Ion Mass Spectrometry (SIMS) on the Sensitive High Resolution Ion MicroProbe-Reverse Geometry (SHRIMP-RG) at the Stanford USGS Micro Analysis Center. Subsequently, 23 of the dated zircons from five samples were selected for oxygen and hafnium isotopic measurements, and analyzed for oxygen at UCLA using SIMS (Cameca IMS-1270) and for hafnium at WSU Geoanalytical Lab using laser ablation-inductively coupled plasma-mass spectrometry (LA-ICP-MS). Standard methodologies of the respective laboratories were used during analyses, which were carried out under the supervision of respective laboratory personnel. Due to the limited zircon yields from individual samples, sandstone xenolith zircon populations were too small for standard detrital zircon geochronology methods (i.e., analyzing 100 grains per sample), but are included here as preliminary data.

Results and interpretations

Zircon U–Pb geochronology data from the samples are shown in Table 1. Oxygen and hafnium isotope data are shown in Tables 2 and 3, respectively. The following abbreviations/notations are used in the presentation of the results: MSWD, mean square of weighted deviates; $\delta^{18}O$ (VSMOW), $^{18}O/^{16}O$ of unknown relative to Vienna Standard Mean Ocean Water *measured per mil* [21]; $\varepsilon Hf_{(i)}$, $^{176}Hf/^{177}Hf$ of unknown relative to chondritic uniform reservoir at the time of zircon crystallization *measured in epsilon units* [22].

Two xenolith samples are fine- to medium-grained plagiogranitic gneisses (samples ZH38 and ZH13). They have weakly foliated texture, are composed of quartz, plagioclase ($An_{27–32}$), and potassium feldspar, but do not have mica in thin section. SHRIMP-RG zircon U–Pb crystallization ages ($n = 32$) from these plagiogranite xenoliths range from 600 to 660 Ma. Three zircons have older cores with $^{207}Pb/^{206}Pb$ ages ranging from 1.47 to 1.88 Ga. Five zircons of Neoproterozoic age have concordant $^{206}Pb/^{238}U$ and $^{207}Pb/^{206}Pb$ ages (discordance (D) < 5 %, Table 1) with $^{206}Pb/^{238}U$ ages ranging from ca. 630–650 Ma. All Neoproterozoic zircon results from this sample combined yield a ^{204}Pb-corrected $^{206}Pb/^{238}$

Table 1 SIMS (SHRIMP-RG) zircon U–Pb ages from xenoliths of Zhokhov Island

No spot	% $^{206}Pb_c$	ppm U	ppm Th	(1)$^{206}Pb/^{238}U$ age, Ma		(1)$^{207}Pb/^{206}Pb$ age, Ma		% Discordance	Total $^{238}U/^{206}Pb$	±%	Total$^{207}Pb/^{206}Pb$	±%	$^{207}Pb^*/^{235}U$	±%	(1) $^{206}Pb^*/^{238}U$	±%	err corr
Sample ZH38 (plagiogranitic gneiss, 152.754° E; 76.1501° N)																	
7	**0.23**	**51**	**3**	**540**	**±8**	**554**	**±75**	**+3**	**11.42**	**1.6**	**0.060**	**2.3**	**0.707**	**3.8**	**0.0874**	**1.6**	**0.4**
6	0.76	17	9	596	±13	406	±284	−49	10.19	2.2	0.066	3.4	0.733	12.9	0.0968	2.3	0.2
16	0.04	47	19	598	±9	353	±127	−72	10.21	1.5	0.060	1.9	0.718	5.8	0.0971	1.6	0.3
15	0.05	110	195	607	±7	678	±44	+11	10.16	1.3	0.060	1.4	0.845	2.4	0.0987	1.3	0.5
19	0.06	52	32	606	±9	250	±174	−150	10.03	1.5	0.060	2.1	0.696	7.7	0.0985	1.6	0.2
17	–	20	13	605	±12	174	±295	−261	10.05	2.1	0.058	5.5	0.672	12.8	0.0984	2.2	0.2
10	0.06	34	23	614	±10	493	±119	−26	9.97	1.7	0.060	2.5	0.786	5.7	0.0998	1.8	0.3
13	–	14	8	622	±15	869	±213	+30	9.98	2.4	0.058	4.2	0.951	10.6	0.1014	2.6	0.2
14	–	329	66	622	±8	559	±20	−12	9.87	1.3	0.059	0.9	0.821	1.6	0.1013	1.3	0.8
3	0.29	25	19	622	±12	426	±194	−48	9.78	1.9	0.063	2.9	0.773	8.9	0.1013	2.0	0.2
4	0.46	96	93	631	±11	736	±38	+15	9.72	1.8	0.064	1.5	0.905	2.5	0.1028	1.8	0.7
12	0.00	87	83	628	±8	574	±78	−10	9.76	1.4	0.060	3.0	0.835	3.8	0.1023	1.4	0.4
8	**0.05**	**964**	**875**	**629**	**±11**	**634**	**±11**	**+1**	**9.75**	**1.8**	**0.061**	**0.5**	**0.860**	**1.9**	**0.1025**	**1.8**	**1.0**
1	1.40	30	19	633	±11	691	±182	+9	9.58	1.8	0.072	2.7	0.889	8.7	0.1031	1.9	0.2
9	**0.05**	**206**	**52**	**637**	**±7**	**641**	**±24**	**+1**	**9.63**	**1.2**	**0.061**	**1.0**	**0.875**	**1.6**	**0.1038**	**1.2**	**0.7**
18	**–**	**345**	**97**	**638**	**±11**	**632**	**±36**	**−1**	**9.61**	**1.8**	**0.060**	**1.7**	**0.872**	**2.5**	**0.1040**	**1.8**	**0.7**
11	–	136	62	639	±10	448	±63	−45	9.55	1.7	0.059	1.3	0.804	3.3	0.1042	1.7	0.5
20	**0.06**	**425**	**99**	**644**	**±10**	**665**	**±17**	**+3**	**9.51**	**1.6**	**0.061**	**0.7**	**0.896**	**1.7**	**0.1051**	**1.6**	**0.9**
21	–	36	29	643	±11	505	±112	−29	9.49	1.7	0.061	2.4	0.830	5.4	0.1049	1.7	0.3
2	**–**	**162**	**188**	**647**	**±16**	**620**	**±59**	**−5**	**9.46**	**2.5**	**0.061**	**2.6**	**0.880**	**3.7**	**0.1056**	**2.5**	**0.7**
5	–	630	12	662	±8	607	±11	−9	9.25	1.3	0.060	0.5	0.896	1.4	0.1081	1.3	0.9
23	**–**	**188**	**59**	**1495**	**±19**	**1474**	**±13**	**−2**	**3.83**	**1.4**	**0.093**	**0.5**	**3.325**	**1.6**	**0.2610**	**1.4**	**0.9**
22	**–**	**292**	**166**	**1743**	**±22**	**1700**	**±25**	**−3**	**3.22**	**1.4**	**0.105**	**1.3**	**4.462**	**2.0**	**0.3104**	**1.4**	**0.7**
Sample ZH13 (plagiogranitic gneiss, 152.8209° E; 76.0917° N)																	
9	-0.36	5074	498	700	±9	597	±7	−18	8.72	1.3	0.060	0.3	0.946	1.4	0.1147	1.3	1.0
6	-0.45	3813	268	724	±10	600	±10	−22	8.41	1.4	0.060	0.5	0.982	1.5	0.1189	1.4	0.9
1	**0.29**	**302**	**133**	**613**	**±133**	**602**	**±32**	**−2**	**9.99**	**22.8**	**0.063**	**0.9**	**0.825**	**22.8**	**0.0998**	**22.8**	**1.0**
5	−0.42	1691	318	735	±32	618	±50	−20	8.28	4.6	0.060	2.3	1.006	5.2	0.1207	4.6	0.9
3	**−0.02**	**4143**	**490**	**626**	**±17**	**621**	**±6**	**−1**	**9.81**	**2.9**	**0.060**	**0.3**	**0.850**	**2.9**	**0.1019**	**2.9**	**1.0**
4	−0.35	2834	1265	717	±16	621	±15	−16	8.50	2.4	0.0605	0.7	0.982	2.5	0.1177	2.4	1.0
7	**−0.03**	**1011**	**160**	**634**	**±8**	**624**	**±10**	**−2**	**9.67**	**1.3**	**0.061**	**0.5**	**0.864**	**1.4**	**0.1034**	**1.3**	**0.9**
8	**−0.04**	**788**	**107**	**648**	**±9**	**633**	**±12**	**−3**	**9.45**	**1.5**	**0.061**	**0.5**	**0.888**	**1.6**	**0.1058**	**1.5**	**0.9**
2	**−0.33**	**89**	**68**	**1880**	**±22**	**1836**	**±13**	**−3**	**2.95**	**1.4**	**0.112**	**0.7**	**5.241**	**1.5**	**0.3385**	**1.4**	**0.9**
Sample ZH1 (sandstone, 152.8469° E; 76.1496° N)																	
9	−0.41	397	144	214	±2				29.4	1.2	0.047	2.4	0.20	4.7	0.034	1.2	0.2
6	−0.71	326	233	250	±2				25.2	1.0	0.046	2.6	0.23	4.8	0.040	1.0	0.2

Table 1 continued

No spot	% $^{206}Pb_c$	ppm U	ppm Th	(1)$^{206}Pb/^{238}U$ age, Ma		(1)$^{207}Pb/^{206}Pb$ age, Ma		% Discordance	Total $^{238}U/^{206}Pb$	±%	Total$^{207}Pb/^{206}Pb$	±%	$^{207}Pb^*/^{235}U$	±%	(1) $^{206}Pb^*/^{238}U$	±%	**err corr**
2	−0.93	81	33	282	±8				22.0	2.6	0.045	5.1	0.20	20.5	0.045	2.7	0.1
5	−0.67	91	65	312	±8				20.1	2.6	0.047	4.6	0.31	8.0	0.050	2.6	0.3
3	−0.53	215	118	375	±7				16.6	1.9	0.050	2.7	0.37	6.4	0.060	1.9	0.3
8	−0.53	525	6	605	±7	431	±27	−43	10.2	1.2	0.056	1.1	0.75	1.7	0.098	1.2	0.7
4	−0.87	971	16	635	±5	330	±24	−97	9.7	0.8	0.054	0.9	0.76	1.4	0.103	0.8	0.6
1	−0.38	64	46	931	±14	706	±93	−34	6.4	1.6	0.067	2.5	1.35	4.7	0.155	1.6	0.3
7	−1.52	84	22	1511	±18	1248	±82	−24	3.8	1.4	0.082	4.2	2.99	4.4	0.264	1.4	0.3
Sample ZH25 (sandstone, 152.8125° E; 76.1596° N)																	
1	−0.21	506	434	161	±1				39.5	0.9	0.048	2.6	0.16	3.9	0.025	0.9	0.2
3	−0.65	179	141	275	±3				22.7	1.2	0.047	3.2	0.24	8.9	0.044	1.2	0.1
2	−0.38	456	119	303	±3				20.7	0.9	0.050	1.9	0.32	3.0	0.048	0.9	0.3
8	−1.11	106	48	303	±4				20.8	1.3	0.043	4.5	0.29	4.7	0.048	1.3	0.3
6	−0.65	666	165	314	±4				20.0	1.2	0.048	3.1	0.32	3.5	0.050	1.2	0.4
4	−0.89	182	105	364	±4				17.1	1.1	0.047	2.9	0.33	6.8	0.058	1.1	0.2
10	−0.62	858	638	418	±3				14.9	0.8	0.050	1.3	0.46	1.7	0.067	0.8	0.5
5	−0.98	117	68	638	±11				9.6	1.8	0.053	2.5	0.70	5.2	0.104	1.9	0.4
7	−0.21	331	207	1102	±10	1012	±25	−10	5.4	1.0	0.075	1.0	1.88	1.6	0.186	1.0	0.6
9	−0.92	114	124	1431	±16	1252	±31	−16	4.0	1.3	0.083	1.4	2.82	2.0	0.249	1.3	0.6
Sample ZH29 (sandstone, 152.5606° E; 76.151° N)																	
1	0.14	1023	445	459	±14				13.5	3.2	0.057	7.2	0.53	9.6	0.074	3.2	0.3
9	−0.75	211	63	1010	±18	799	±71	−29	5.9	2.0	0.067	3.2	1.54	3.9	0.170	2.0	0.5
2	−1.11	94	42	1141	±14	781	±67	−50	5.1	1.4	0.069	1.9	1.74	3.5	0.194	1.4	0.4
7	−0.84	203	57	1163	±11	956	±56	−24	5.1	1.1	0.072	2.6	1.93	2.9	0.198	1.1	0.4
8	−0.28	349	71	1169	±10	1041	±42	−13	5.0	0.9	0.077	1.8	2.03	2.3	0.199	0.9	0.4
4	−1.44	228	112	1205	±23	860	±34	−44	4.9	2.1	0.069	1.4	1.92	2.6	0.206	2.1	0.8
5	−0.68	107	54	1290	±15	1126	±55	−16	4.5	1.3	0.079	2.5	2.36	3.0	0.222	1.3	0.4
6	−0.94	136	72	1419	±37	1235	±30	−17	4.1	2.9	0.082	1.4	2.77	3.3	0.246	2.9	0.9
3	−1.29	90	68	1673	±20	1479	±26	−15	3.4	1.4	0.093	1.4	3.78	1.9	0.296	1.4	0.7
Sample ZH28 (sandstone, 152.5606° E; 76.151° N)																	
2	0.13	580	415	308	±10				20.3	3.5	0.054	5.3	0.33	7.3	0.049	3.5	0.5
3	−0.74	285	117	426	±4				14.5	1.0	0.050	2.0	0.42	4.4	0.068	1.0	0.2
1	−0.80	272	308	1766	±16	1654	±57	−8	3.2	1.0	0.102	3.1	4.42	3.2	0.315	1.0	0.3

Errors shown as 1σ, $^{206}Pb_c$, common led. Error in Temora standard calibration was 0.45%. *(1)* ages corrected to measured ^{204}Pb. *D* discordance between $^{206}Pb/^{238}U$ and $^{207}Pb/^{206}Pb$ ages for $^{206}Pb/^{236}U$ ages > 500 Ma. Bold shows zircons with $D < 6\%$

Table 2 SIMS oxygen isotopic composition of zircons from granitic gneiss crustal xenolith (sample ZH38) of Zhokhov Island

No spot	^{16}O	^{16}O err	^{18}O	^{18}O err	$^{18}O/^{16}O$	err	$\delta^{18}O$ meas ‰	err	$\delta^{18}O$ VSMOW ‰	err
1	2.99E+09	4.37E+05	6.01E+06	8.92E+02	2.01E–03	9.12E–08	3.82	0.05	3.52	0.22
2	3.00E+09	7.64E+05	6.05E+06	1.55E+03	2.01E–03	1.25E–07	5.26	0.06	4.84	0.30
3	2.93E+09	8.97E+05	5.90E+06	1.80E+03	2.01E–03	1.25E–07	3.47	0.06	3.19	0.20
4	2.99E+09	7.65E+05	6.02E+06	1.43E+03	2.01E–03	1.72E–07	3.79	0.09	3.49	0.23
5	3.00E+09	2.60E+06	6.03E+06	5.23E+03	2.01E–03	1.13E–07	4.19	0.06	3.86	0.24
6	2.97E+09	3.59E+05	5.97E+06	8.32E+02	2.01E–03	1.42E–07	2.67	0.07	2.46	0.16
7	2.96E+09	1.08E+06	5.96E+06	2.19E+03	2.01E–03	1.24E–07	4.00	0.06	3.68	0.23
8	2.98E+09	5.67E+05	5.99E+06	1.16E+03	2.01E–03	8.56E–08	3.38	0.04	3.11	0.19

err error as 2 sigma, error in standard R33 = 0.06 %; correction factor using standard 91500 = 1.024844

Table 3 LA-ICPMS Hf isotope results from zircons separated from crustal xenoliths of Zhokhov Island

Sample_spot	$^{176}Hf/^{177}Hf_{(m)}$	$^{176}Hf/^{177}Hf_{(cor)}$	±2σ	$^{206}Pb/^{238}U$ age	$^{176}Hf/^{177}Hf_{(i)}$	εHf_0	εHf_i	±2σ
Sample ZH38 (plagiogranitic gneiss, 152.754° E; 76.1501° N)								
ZH38_8	0.282667	0.282709	5.1E–05	629	0.282668	−4.2	9.9	1.8
ZH38_9	0.282721	0.282763	2.6E–05	637	0.282738	−2.3	12.6	0.9
ZH38_5	0.282697	0.282739	2.3E–05	662	0.282724	−3.1	12.6	0.8
ZH38_4	0.282735	0.282777	2.8E–05	631	0.282741	−1.8	12.5	1.0
ZH38_3	0.282712	0.282754	3.0E–05	622	0.282730	−2.6	12.0	1.1
ZH38_1	0.282716	0.282758	2.5E–05	633	0.282739	−2.4	12.5	0.9
Sample ZH13 (plagiogranitic gneiss, 152.8209° E; 76.0917° N)								
ZH13_7	0.282634	0.282676	4.1E–05	634	0.282653	−5.3	9.5	1.5
ZH13_6	0.282618	0.282660	2.7E–05	724	0.282637	−5.9	11.0	1.0
ZH13_2	0.281575	0.281617	4.1E–05	1880	0.281585	−42.8	0.0	1.5
ZH13_1	0.282658	0.282700	3.0E–05	613	0.282687	−4.5	10.2	1.1
Sample ZH1 (sandstone, 152.8469° E; 76.1496° N)								
ZH1_1	0.282225	0.282267	5.7E–05	931	0.282257	−19.8	2.2	2.0
ZH1_4	0.281284	0.281326	4.8E–05	635	0.281319	−53.1	−37.7	1.7
ZH1_6	0.282561	0.282603	3.4E–05	250	0.282598	−7.9	−1.1	1.2
ZH1_7	0.281887	0.281929	4.1E–05	1511	0.281916	−31.8	3.3	1.5
Sample ZH25 (sandstone, 152.8125° E; 76.1596° N)								
ZH25_10	0.282621	0.282663	3.4E–05	418	0.282652	−5.8	4.6	1.2
ZH25_9	0.281787	0.281829	4.4E–05	1431	0.281803	−35.3	−2.6	1.6
ZH25_8	0.282623	0.282665	4.0E–05	303	0.282661	−5.7	2.4	1.4
ZH25_5	0.282494	0.282536	4.0E–05	638	0.282530	−10.3	5.2	1.4
ZH25_6	0.282582	0.282624	3.9E–05	314	0.282618	−7.2	1.1	1.4
ZH25_3	0.282380	0.282422	3.1E–05	275	0.282416	−14.3	−6.9	1.1
ZH25_2	0.282442	0.282484	3.3E–05	303	0.282482	−12.1	−4.0	1.2
ZH25_1	0.282365	0.282407	3.9E–05	161	0.282403	−14.9	−9.9	1.4
Sample ZH29 (sandstone, 152.5606° E; 76.151° N)								
ZH29_1	0.282593	0.282635	3.5E–05	459	0.282621	−6.8	4.4	1.2
ZH29_9	0.282086	0.282128	3.7E–05	1010	0.282120	−24.7	−0.9	1.3
ZH29_8	0.282192	0.282234	2.9E–05	1169	0.282218	−21.0	6.2	1.0
ZH29_7	0.282047	0.282089	4.8E–05	1163	0.282079	−26.1	1.1	1.7
ZH29_4	0.282100	0.282142	2.6E–05	1205	0.282126	−24.2	3.7	0.9

^{176} $Hf/^{177}Hf_{(m)}$ measured ratio, $^{176}Hf/^{177}Hf_{(corr)}$ corrected on standard ratio, $^{176}Hf/^{177}Hf_{(i)}$ initial ratio in accordance with U–Pb age

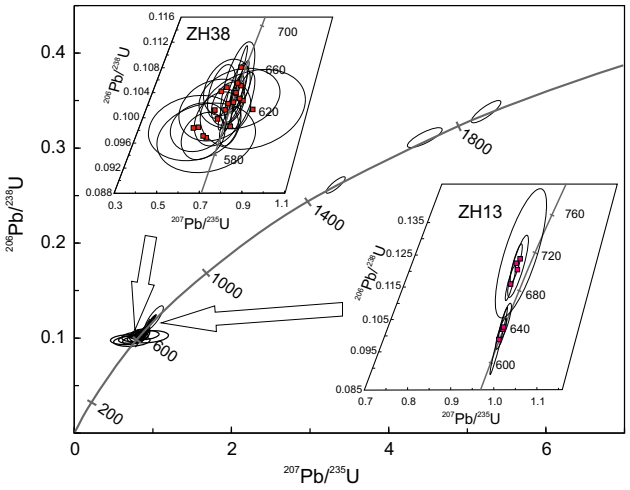

Fig. 3 U–Pb Concordia diagram for zircons from Zhokhov plagiogranite-gneiss xenoliths (samples ZH38 and ZH13) with zoomed inset showing data for Neoproterozoic cluster (^{204}Pb corrected isotopic ratios). *Error ellipses* are plotted at 2-sigma uncertainty

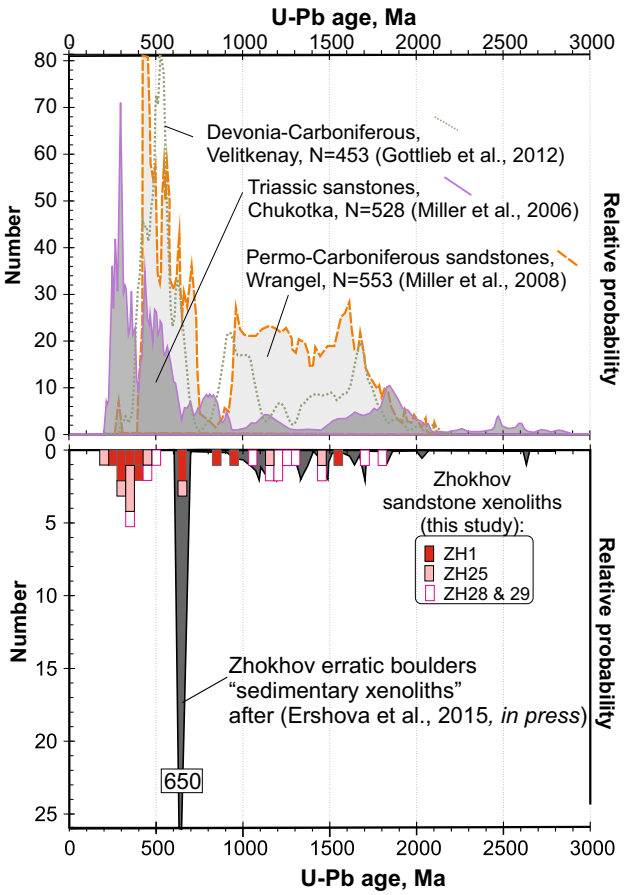

Fig. 4 Comparison of published detrital zircon populations from Arctic Chukotka sandstones of different ages [6, 13, 14] with Zhokhov sandstone xenoliths obtained in this study. Zhokhov boulder erratics referred as "sandstone xenoliths" from (Ershova et al. [4] in press) are shown for comparison. Probability density curves are created using Isoplot 3.0

U-weighted mean age of 626 ± 9 Ma (2σ, MSWD = 3.4, $N = 23$; Fig. 3). Three concordant ($D < 3$ %) zircons from sample ZH13 yield ^{204}Pb-corrected ^{206}Pb/^{238}U-weighted mean age of 638 ± 11 Ma (2σ, MSWD = 1.0), within error of the ZH38 result (Fig. 3). The high MSWD value in ZH38 casts significant uncertainty on interpreting the mean age as reflecting a single magmatic event, although the range of ages from 600 to 660 Ma likely reflects the timespan of magmatism and associated high temperature metamorphism in the crust. However, zircons from xenoliths theoretically may have experienced lead loss while they were transported by hot basaltic melt, and large dispersion of individual U–Pb ages indicates this may be a possibility (Fig. 3). However, seven zircons yield near concordant ^{206}Pb/^{238}U and ^{207}Pb/^{206}Pb ages (discordance < 5 %, Table 1) and discordant results do not exhibit a coherent trend toward a Pliocene lower intercept age on concordia (the age of the enclosing basalt).

The oxygen isotopic composition of dated zircons from sample ZH38 shows a range of δ^{18}O (VSMOW) from 4.8 to 2.5 ‰ (weighted mean 3.3 ± 0.5 ‰) (Table 2) attaining mantle values when zircon values are recalculated to whole rocks data [21]. Hf isotopic composition of late Neoproterozoic zircons is similar to modeled depleted mantle values with $\varepsilon Hf_{(i)}$ ranges from +9.9 to +12.6, and ^{176}Hf/^{177}Hf$_{(i)}$ from 0.282668 to 0.282741 (Table 3, Fig. 5). These results yield Lu–Hf model ages of 740–880 Ma for extraction from depleted mantle, assuming average crustal value of ^{176}Lu/^{177}Hf = 0.0093 [22].

Three sandstone xenoliths (ZH1, ZH25, ZH29) that we studied exhibit varied lithology and detrital zircon spectra, suggesting not all sandstone xenoliths were derived from the same stratigraphic interval. Sample ZH29 is a grayish brown fine-grained subangular, slightly feldspathic quartz-rich sandstone cemented by small amount of clay matrix containing small fragments of partially melted mica and potassium feldspar. Eight zircon grains from this sandstone yield ^{207}Pb/^{206}Pb ages of 1.0–1.6 Ga, and one grain yielded a ^{206}Pb/^{238}U age of 460 ± 14 Ma. Hafnium isotopic composition of six dated zircons have a broad range ($\varepsilon Hf_{(i)}$ from −0.9 ± 1.3 to +6.2 ± 1; Table 3; Fig. 5).

Samples ZH1 and ZH25 are light gray, fine-grained, subangular, weakly cemented sandstones which are partially melted near the contact with the host lava. They are composed of quartz (~50–60 %), feldspar (~10–20 %), and partially melted clay matrix. Seven detrital zircon grains from sample ZH1 yield ages that range from Proterozoic to Permian (five grains ages are Carboniferous to Permian), suggesting a maximum depositional age of latest Paleozoic or younger (Fig. 4; Table 1). Ten detrital zircon grains from sample ZH25 yield results similar to the ZH1 age distribution pattern, with predominantly

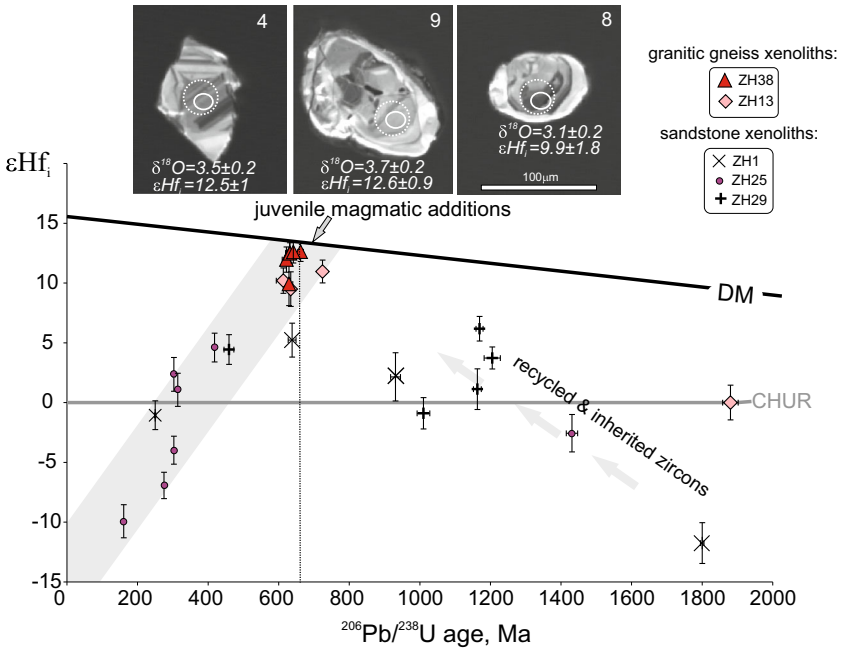

Fig. 5 Time versus $\varepsilon Hf_{(i)}$ for zircons from crustal xenoliths of Zhokhov Island showing possible late Neoproterozoic depleted juvenile magmatic additions and isotopic evolution of crust during Phanerozoic. *Photographs at the top*—CL images of zircons from plagiogranite-gneiss xenolith (sample ZH38), *circled* are analyzed points for oxygen and hafnium isotopic composition. *Points numbers* in upper right corners as in Tables 1 and 3

Carboniferous to Permian ages. The youngest zircon from ZH25 yields a $^{206}Pb/^{238}U$ age of 216 ± 2 Ma, whereas one grain from ZH1 exhibits concordant $^{206}Pb/^{238}U$ and $^{208}Pb/^{232}Th$ ages around 160 Ma. Given that only one Mesozoic age result was obtained from each sample, it is difficult to substantiate whether these zircons reflect derivation from a Mesozoic (or younger) sedimentary rocks or whether they are simply spurious age results. The ubiquity of Late Jurassic and Early Cretaceous age sandstones across the AACM which contain Triassic and Jurassic age zircons (e.g., [14]) suggests there could be a geologic analog to the sandstones represented by these small xenoliths, although more data are clearly needed to evaluate any potential relationships. $\varepsilon Hf_{(i)}$ in eight dated Phanerozoic zircons from samples ZH1 and ZH25 ranges broadly from +4.6 to −9.9 ± 1.4, and trend away from juvenile depleted magmatic zircons (ZH38 and 13) when plotted as $\varepsilon Hf_{(i)}$ versus time (Table 3; Fig. 5).

In summary, zircons from granitic gneiss xenoliths are Neoproterozoic with U–Pb protolith ages ca. 660–600 Ma, and have depleted mantle-like Hf isotopic signatures and yield near (slightly lighter than) mantle $^{18}O/^{16}O$ isotope ratios in zircon. Initial Hf isotopic compositions of dated zircons from magmatic and sedimentary rocks are consistent with formation/addition of juvenile crust in Neoproterozoic time followed by reworking of the crust (without additional juvenile input) during Phanerozoic time. U–Pb ages and Hf model ages obtained here are similar to widespread pre-Uralian–Timanian magmatic arc basement exposed west of the Ural Mountains [10, 15, 18] and are similar to protolith ages for granite intrusions and orthogneiss dated along the Arctic coast of Chukotka [2, 6].

Implications

The limited number of detrital zircons dated from the small sandstone xenoliths and the limited stratigraphic knowledge about the subsurface of Zhokhov Island are problematic in terms of using this data for meaningful paleogeographic interpretations. However, the robust and rapidly growing database of circum-Arctic detrital zircon spectra (e.g., [4, 13–16, 18]) provides a framework for a preliminary comparison of the data reported here to that elsewhere using histograms and probability density plots. Figure 4 illustrates that the zircons from Zhokhov sandstone xenoliths predominantly yield Carboniferous to Triassic age results, similar to Mesozoic sandstones of the Russian Arctic [13, 14, 16].

Some useful comparisons can be made between these new xenolith zircon age data and recently published geochronology from other De Long archipelago samples. Zircons from an quartz-rich sandstone boulder erratic on Zhokhov ([4, 12] and sandstone Unit B from nearby Henrietta Island [4]) exhibit late Neoproterozoic age peaks ca. 590–660 Ma, similar to the age of Zhokhov Island Neoproterozoic granitoid xenoliths and the spectra of detrital zircon ages in some of our sandstone xenoliths (Fig. 4). By contrast, a second quartz-rich sandstone boulder erratic from Zhokhov Island yielded a younger ca. 550 Ma peak, similar in age to the age of granitic

boulder erratics collected in the same locality by Lorenz [12]. In comparison, ca. 550 Ma zircon ages are rare in the granitic and sandstone xenoliths analyzed in this study. In aggregate, the detrital zircon populations in sandstone boulder erratics on Zhokhov and Henrietta Islands yield ages that are characteristic of pre-Uralian–Timanian magmatic rocks and clastic strata weathered from them. The zircon populations in sandstone xenoliths we present here are clearly derived from younger rocks or strata.

Our basement geochronology suggests an age affinity between Zhokhov Island and the basement of Arctida [23] that was accreted to Baltica in the Timanian orogeny (e.g., [5, 10]. Our data for the cover sequences are compatible with basement ages—the sediments have detrital signatures similar to Permian and Triassic sequences of the Urals, West-Siberia Basin, and Taimyr region. These sedimentary sequences would postdate the Uralian orogeny that brought Siberia to Baltica and/or Timanides [4, 18]. They also provide enhanced ties with strata this age in Chukotka that have been shown to have been derived from this same general region in Triassic time [16].

In conclusion, we suggest that crustal xenoliths from Zhokhov Island were plucked from shallow crustal depths from the basement beneath the basalt flows of the De Long archipelago, where the subsurface geology, based on this data, is likely to be comprised of late Neoproterozoic granitic gneisses and Phanerozoic sedimentary cover perhaps as young as Triassic or Jurassic (?) Accordingly, the basement rocks of Zhokhov Island are linked to, and autochthonous, with respect to, the northern Timanide region of Baltica upon closure of the Eurasia Basin (Fig. 1). The inferred basement beneath Zhokhov Island is also correlative to that of parts of the Arctic Alaska–Chukotka continental block. The Hf isotopic data from Zhokhov Island zircons indicate the rocks analyzed represent juvenile magmatic additions during the latter Neoproterozoic (roughly correlated with the breakup of Rodinia and coeval plume-related magmatism) and are consistent with the reworking of this isotopically evolving crustal reservoir during Paleozoic and Mesozoic magmatism and crustal modification/maturation.

Acknowledgments V.V. Akinin thanks VSEGEI for the opportunity to participate in the Arctic expedition to Zhokhov Island. P. O. Sobolev and C.V. Yudin C.V provided assistance during the field trip. We thank M. Coble, A. Schmitt, R. Economos, J. Vervoort, C. Fisher, and C. Knaack for providing access and expertise for analytical work. We appreciate the reviewers for useful suggestions. Travel and analytical expenses were supported partly by RFBR grant 16-05-00949, DVO RAS (15-I-1-008), and CRDF (RUG1-7089-XX-13). This material is based upon work supported by the National Science Foundation under grant NSF-EAR 0948673 (Miller). This also represents a contribution to the international Circum Artic Lithospheric Evolution consortium.

References

1. Akinin VV, Andronikov AV, Mukasa SB, Miller EL (2013) Cretaceous lower crust of the continental margins of the northern Pacific: petrologic and geochronologic data on lower to middle crustal xenoliths. Petrology 21:34–73. doi:10.1134/S0869591113010013
2. Amato JM, Aleinikoff JN, Akinin VV, McClelland WC, Toro J (2014) Age, chemistry, and correlations of Neoproterozoic-Devonian igneous rocks of the Arctic Alaska-Chukotka terrane: an overview with new U-Pb ages. In: Till AB, Dumoulin JA (eds) Reconstruction of a Late Proterozoic to Devonian continental margin sequence, northern Alaska, its paleogeographic significance, and contained base-metal sulfide deposits, GSA Special Paper 506. doi:10.1130/2014.2506
3. Churkin M Jr, Whitney JW, and Rogers JF (1985) The North American–Siberian connection, a mosaic of craton fragments in a matrix of oceanic terranes. In: Howell DG (ed.) Tectonostratigraphic Terranes of the Circum-Pacific Region, Earth Science Series 1. Circum-Pacific Council for Energy and Mineral Resources, Texas, pp 79–84
4. Ershova VB, Lorenz, H, Prokopiev AV, Sobolev NN, Khudoley AK, Petrov EO, Estrada S, Sergeev S, Larionov A, Thomsen TB (2015, in press) The De Long Islands: a missing link in unraveling the Paleozoic paleogeography of the Arctic, Gondwana Res. doi:10.1016/j.gr.2015.05.016
5. Gee DG, Pease V (eds) (2004) The neoproterozoic timanide orogen of eastern Baltica. Geological Society, vol 30. London, Memoirs
6. Gottlieb ES, Miller EL, Akinin VV (2012) Crustal architecture of Arctic Chukotka revealed by field mapping and zircon U-Pb geochronology. EOS Trans AGU, Fall Meet Suppl, ID 1492847
7. Jakobbson M, Andreassen K, Bjarnadóttir LR, Dove D, Dowdeswell JA, England JH, Funder S, Hogan K, Ingólfsson Ó, Jennings A, Larsen NK, Kirchner N, Landvik JY, Mayer L, Mikkelsen N, Möller P, Niessen F, Nilsson J, O'Regan M, Polyak L, Nørgaard-Pedersen N, Stein R (2014) Arctic Ocean glacial history. Quaternary Sci Rev 92:40–67
8. Korago EA, Vernikovsky VA, Sobolev NN, Larionov AN, Sergeev SA, Stolbov NM, Proskurin VF, Sobolev PS, Metelkin DV, Matushkin NY, Travin AV (2014) Age of the basement beneath the De Long Islands (New Siberian Archipelago): New geochrological data. Dokl Earth Sci 457:803–809
9. Kos'ko MK, Cecile MP, Harrison JC, Ganelin VG, Khandoshko NV, Lopatin BG (1993) Geology of Wrangel Island, between Chukchi and East Siberian seas, northeastern Russia. Geol Surv Can Bull 461:1–107
10. Kuznetsov NB, Natapov LM, Belousova EA, O'Reilly SY, Griffin WL (2010) Geochronological, geochemical and isotopic study of detrital zircon suites from late Neoproterozoic clastic strata along the NE margin of the East European Craton: implications for plate tectonic models. Gondwana Res 17(2/3): 583–601
11. Layer P, Parfenov LM, Surnin AA et al (1993) First 40Ar/39Ar age estimation on magmatic and metamorphic rocks of Verkhoyansk-Kolyma mesozoides. Dokl Earth Sci 329(5):621–624
12. Lorenz H. (2013) Geochronology of crustal xenoliths and detrital zircons from the De Long islands. 3P Arctic conference and exhibition, Stavanger, Norway, abstract 90177
13. Miller EL, Toro J, Gehrels G, Amato JM, Prokopiev A, Tuchkova MI, Akinin VV, Dumitru TA, Moore TE, Cecile MP (2006) New

insights into Arctic paleogeography and tectonics from U-Pb detrital zircon geochronology. Tectonics. doi:10.1029/2005TC001830
14. Miller EL, Soloviev A, Kuzmichev A, Gehrels G, Toro J, Tuchkova M (2008) Jurassic and Cretaceous foreland basin deposits of the Russian Arctic: Separated by birth of the Makarov Basin? Norw J Geol 88:201–226
15. Miller EL, Kuznetsov N, Soboleva A, Udoratina O, Grove MJ, Gehrels G (2011) Baltica in the Cordillera? Geology 39:791–794
16. Miller EL, Soloviev AV, Prokopiev AV, Toro J, Harris D, Kuzmichev AB, Gehrels GE (2013) Triassic river systems and the paleo-Pacific margin of northwestern Pangea. Gondwana Res 23:1631–1645
17. Natal'in BA, Amato JM, Toro J, Wright JE (1999) Paleozoic rocks of northern Chukotka Peninsula, Russian Far East: Implications for the tectonics of the Arctic region. Tectonics 18:977–1003
18. Pease VL, Kuzmichev AB, Danukalova MK (2014) The New Siberian Island and evidence for the continuation of the Uralides, Arctic Russia. J Geol Soc Lond 172:1–4
19. Savostin LA, Silantyev SA, Bogdanovsky OG (1988) New data on volcanism of Zhokhova Island (De-Longa archipelago). Dokl Acad Nauk SSSR 302(6):1443–1447 **(in Russian)**
20. Silantyev SA, Bogdanovskii OG, Fedorov PI, Karpenko SF, Kostitsyn YA (2004) Intraplate magmatism of the De Long Islands: a response to the propagation of the ultraslow-spreading Gakkel Ridge into the passive continental margin in the Laptev Sea. Russ J Earth Sci 6(3):153–183
21. Valley JW (2003) Oxygen isotopes in zircon. In: Hanchar JM, Hoskin PWO (eds) Zircon. Reviews in mineralogy and geochemistry, vol 53. Mineralogical Society of America, Washington, pp 343–386
22. Vervoort JD, Patchett PJ (1996) Behavior of hafnium and neodymium isotopes in the crust: constraints from Precambrian crustally derived granites. Geochim Cosmochim Ac 60:3717–3733
23. Zonenshain LP, Kuz'min MI, Natapov LM, Page BM (1990) Geology of the USSR: a plate-tectonic synthesis. Geodinamic Series 21. AGU, Washington